Component Dynamics in Polyisoprene/Polyvinylethylene Blends Well above T_g

Bumchan Min,† XiaoHua Qiu, and M. D. Ediger*

Department of Chemistry, University of Wisconsin−Madison, Madison, Wisconsin 53706

Marinos Pitsikalis and Nikos Hadjichristidis

Department of Chemistry, University of Athens, Panepistimiopolis Zografou 15771 Athens, Greece

Received October 25, 2000

ABSTRACT: ^{13}C and ^{2}H NMR relaxation time measurements were performed on low molecular weight blends of polyisoprene (M_n = 1350 g/mol) and deuterated polyvinylethylene (1,2-polybutadiene; M_n = 2350 g/mol) in order to extract the segmental correlation times for each component. A wide range of temperatures (295−405 K) and several compositions (PI/dPVE: 100/0, 70/30, 50/50, 30/70, and 0/100) were investigated. At high temperatures, dPVE dynamics are 6 times slower than PI dynamics even after considering self-concentration effects. This intrinsic mobility difference is in quantitative agreement with measurements on each chain individually as a dilute component in a common solvent, suggesting a purely intramolecular origin. The reported correlation times at various compositions fit together smoothly with those obtained by Kornfield and co-workers near T_g, thus providing a unified data set for testing models. One model based on local composition fluctuations captures some qualitative features of the experimental data while failing to describe others.

Introduction

In the next generation of materials, polymers will be utilized increasingly as part of multicomponent systems. Examples of these components include solid substrates, fillers, other synthetic polymers or copolymers, and biological structures. In such an environment, the dynamics of segments of one type are influenced by the presence of other segment types or nearby surfaces, and these changes in dynamics will, in turn, influence transport and mechanical properties critical to the function of these composite structures. Miscible polymer blends are an important test of our ability to understand dynamics in multicomponent systems for two reasons. First, because of intimate mixing, each component is strongly influenced by the presence of the other. Second, polymer blends are technologically important,[1] and we can be optimistic that an improved understanding of dynamics in such systems will lead to strategies for dealing with the complex rheological features which these systems exhibit. Indeed, significant progress has already been made along these lines.[2,3]

For a comprehensive understanding of dynamics in miscible polymer blends, it is essential to have data on the segmental dynamics of *both* components over a wide temperature range. Polyisoprene/polyvinylethylene (PI/PVE) is probably the best studied blend system,[4−18] with a slightly negative χ making it miscible at all molecular weights and temperatures.[4−6] Various techniques utilized include thermal analysis, mechanical measurements,[5,12] solid-state ^{1}H NMR, ^{13}C NMR,[7] ^{2}H 2D-NMR,[9,11] quasi-elastic neutron scattering,[16,17] and dielectric spectroscopy.[10,13,16] Dynamics in other blend systems have also been studied extensively.[19−25] Despite these important contributions, we do not yet have data for any blend system on the dynamics of both components at multiple compositions over a wide temperature range. Such data are essential for testing models[15,26−29] or simulations[17] of blend dynamics.

NMR methods based upon isotopic labeling provide a clean separation of component dynamics, and the combination of solid-state and relaxation time measurements provides access to a wide range of time scales ($1-10^{-10}$ s) corresponding to a temperature range from T_g to T_g + 200 K. Solid-state measurements have already been performed on PI/PVE blends by Kornfield and co-workers.[9,11] In this study, we complement this previous work with relaxation time measurements on the PI/PVE system.

We have studied the blend of hydrogenous PI with deuterated PVE, using ^{13}C and ^{2}H NMR respectively to obtain ^{13}C T_1 and NOE and ^{2}H T_1. A wide range of temperatures (295−405 K) and several compositions (PI/dPVE: 100/0, 70/30, 50/50, 30/70, and 0/100) were investigated. For each composition and component, correlation times for segmental dynamics were extracted by fitting T_1 (and NOE) values to the modified Kohlrausch−Williams−Watts correlation function and a VTF temperature dependence. Direct superposition of the experimental data at different compositions gave information about changes in dynamics which was consistent with the fitting procedure.

The major conclusions of our study are as follows. First, at sufficiently high temperature, the segmental dynamics of dPVE are a factor of 6 slower than the PI dynamics while the dynamics of both components are essentially independent of composition. This can only be explained by an intrinsic mobility difference between the two chains. Interestingly, this intrinsic mobility difference can be quantitatively explained on the basis of the segmental dynamics of PI and PVE in dilute solution, suggesting that the observed mobility difference is completely intramolecular in origin. Second, our results at high temperature fit together smoothly with those reported by Kornfield and co-workers near T_g,

* To whom correspondence should be addressed.
† Present address: Samyang Central Research Institute, Daejoen 305-348, Korea.

10.1021/ma0018345 CCC: $20.00
Published on Web 05/24/2001

thus providing a unified data set for testing various models. Finally, when compared with the ratio of segmental relaxation times for PVE and PI from the combined data set, the recent model of Kumar et al.[15] does not quantitatively describe the experimental data but does capture some qualitative features of the results.

The experiments reported here were performed with a narrow molecular weight distribution and relatively low molecular weight chains (M_n = 1350, 2350 g/mol) in order to allow quantitative comparisons with molecular dynamics computer simulations. We anticipate that such comparisons will result in improved simulations and microscopic insight into dynamics in blend systems. Based on comparisons made below, these chains are long enough to exhibit the segmental dynamics of high molecular weight chains in the pure melt state, once differences in T_g are taken into account.

Samples and Methods

Materials. The solvents (benzene and cyclohexane) and isoprene were purified according to standard methods for anionic polymerization.[30] Deuterated butadiene was obtained by the thermal decomposition of the corresponding sulfone at 400 K. The monomer gas was transferred through KOH 20% solutions to remove the SO_2 and condensed in a flask containing CaH_2 at 77 K. Deuterated butadiene was subsequently purified by standing over *n*-butyllithium at 263 K for 30 min twice.[31] *sec*-Butyllithium was prepared under vacuum by the reaction of the corresponding chloride with lithium dispersion. Dipiperidinoethane (dipip) was purified over CaH_2, Na mirror, and Na/K alloy, and the characteristic blue color was obtained.

Synthesis. The synthesis was performed in vacuo in all-glass reactors with break-seals and constrictions. The polymerization of isoprene was conducted in benzene at room temperature. Deuterated butadiene was polymerized in cyclohexane at 273 K using dipip as a microstructure modifier ([dipip]/[CLi] = 4/1).[32] The living polymers were terminated with degassed methanol. Because of the low molecular weight of the samples, a considerable amount of lithium salt was produced by the termination reaction. Therefore, the samples were dissolved in toluene, and the salts were extracted several times with distilled water. The organic phase was dried over anhydrous sodium sulfate, and then the polymers were precipitated in methanol and dried under vacuum. Transparent samples were obtained.

Sample Characterization. SEC experiments were conducted at 313 K using a modular instrument consisting of a Waters model 510 pump, a Waters model U6K sample injector, a Waters model 401 differential refractometer, and a set of 4 m Styragel columns with a continuous porosity range from 10^6 to 500 Å. The columns were housed in an oven thermostated at 313 K. THF was the carrier solvent at a flow rate of 1 mL/min. The number-average molecular weights M_n were obtained using a Jupiter model 833 vapor pressure osmometer (VPO) operating at 323 K. Toluene refluxed over CaH_2 was used as the solvent. The microstructure of the samples was analyzed by ^{1}H and ^{13}C NMR spectroscopy. Differential scanning calorimetry experiments were conducted using a Seiko 220C DSC (Seiko Instruments) coupled with a Seiko DSC 5200 data station. The samples were cooled at a rate of 10K/min to about T_g − 60 K held for 2 min and heated for 10 K/min to about T_g + 30 K. T_g was determined using the midpoint convention. Sample characterization is given in Table 1.

Preparation of Blend Samples. Five different NMR samples (PI/dPVE: 100/0, 70/30, 50/50, 30/70, and 0/100 in wt %) were prepared as follows. First, PI and dPVE were dissolved in cyclopentane to make 10% solutions and mixed in the appropriate proportions for each blend sample. The mixed solution was transferred to an NMR tube, and about $^3/_4$ of the solvent was removed under vacuum. The resulting concentrated solution was physically coated onto the walls of the NMR tube to make a layer less than 1 mm thick. A vacuum was then applied while holding the tube horizontally. After 72 h, the tubes were sealed under vacuum. From inspection of the ^{13}C NMR spectrum, no solvent remained at a level higher than 0.5%. Samples were refrigerated except during sample preparation and measurement to prevent degradation (e.g., cross-linking of dPVE). The measured T_g values of blend samples are presented in Table 2. Several tests were performed to ensure that no significant degradation took place during experimental measurements (typically several hours at each temperature).

Table 1. Characterization of PI and dPVE Samples

properties	samples PI	samples dPVE
M_n (g/mol)[a]	1350	2350
M_w/M_n[b]	1.11	1.05
microstructure[c]	*cis*-1,4: 61% *trans*-1,4: 24% 3,4: 15%	1,2: 94% 1,4: 6%

[a] Number-average molecular weight by VPO in toluene at 323 K. [b] Molecular weight distribution by SEC in THF at 313 K. [c] From ^{13}C NMR.

Table 2. Glass Transition Temperatures of Pure and Blend Samples

samples	pure PI	70/30	50/50	30/70	pure dPVE
T_g (K)	201	207	212	223	260

NMR Relaxation Measurements. Three different relaxation measurements were conducted so that the dynamics of both components could be determined in each sample. All of these NMR observables are sensitive to segmental dynamics as they measure the reorientation of C−H or C−D bond vectors. ^{13}C NMR experiments tell us only about the dynamics of the polyisoprene chains while ^{2}H experiments tell us only about the dynamics of polyvinylethylene. T_1 measurements determine the length of time required for the spin population to return to equilibrium after the spin population is inverted. This time is not directly the time scale for segmental dynamics, but under the conditions of our experiments, T_1 is controlled by segmental dynamics as shown by eqs 1−9. As a qualitative illustration, in the high-temperature region of our experiments, T_1 gets an order of magnitude longer as the segmental dynamics get an order of magnitude faster.

For PI, ^{13}C T_1 and NOE were measured for the three backbone carbons bonded to hydrogens (carbons 1, 3, and 4 in Figure 1) from 295 to 405 K. ^{13}C Larmor frequencies of 25.2 and 125.9 MHz were utilized with Bruker AC-100 and Varian Unity-500 NMR spectrometers. The standard inversion recovery method was used for T_1 with proton decoupling. A total of 12−16 delay times were used to determine the magnetization curves, which were well described by single exponentials. The relaxation delay between each scan was 5 times the longest relaxation time of the carbons of interest. For NOE measurements, the intensity of the spectrum with continuous decoupling was compared with that from inverse gated decoupling. Here the relaxation delay between successive scans was 10 times the longest relaxation time.

To investigate dPVE dynamics, ^{2}H T_1 values were measured at ^{2}H frequencies of 15.4 and 76.8 MHz from 320 to 405 K. ^{2}H T_1 values were also measured by the inversion−recovery method. At lower temperatures and at the lower field, substantial overlap was observed among the four resonance lines. To interpret the data consistently, all ^{2}H NMR spectra were processed by imposing 500 Hz line broadening to generate a single line. The evolution of magnetization was fitted by four exponential functions. Though we could not obtain meaningful individual ^{2}H T_1s from this procedure, reasonable and reproducible rate-averaged T_1 values could be obtained; based on various tests, the measured rate-average T_1 is considered accurate within 10%. The rate-average T_1 is used because this quantity is linear in the spectral density function (see eq 6). For all measurements, temperature was calibrated using an ethylene glycol sample (accuracy of ±2 K) and controlled to ±1 K.

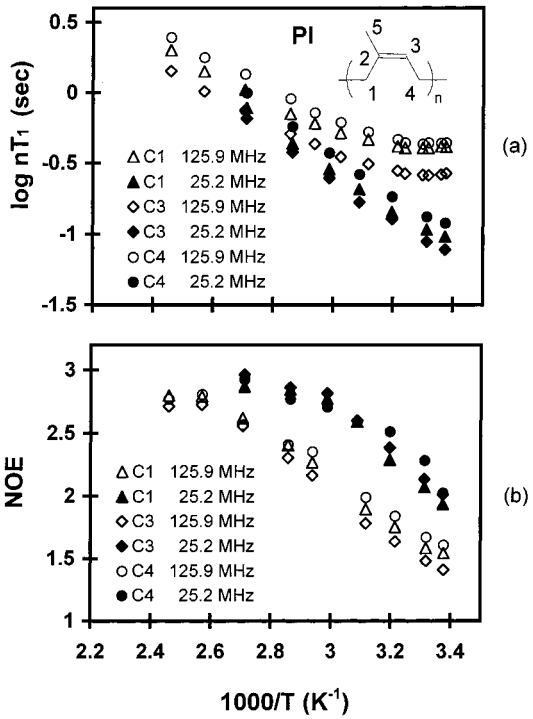

Figure 1. ^{13}C NMR relaxation time measurements for backbone carbons in pure polyisoprene (carbons 1, 3, and 4).

NMR Relaxation Equations. The spin of the ^{13}C nucleus in a $^{13}C-\{^1H\}$ bond has two potential relaxation mechanisms in the investigated systems. Dipole−dipole (DD) coupling is the only significant relaxation process for sp^3 carbons and PI carbons 1 and 4. For sp^2 carbons, the chemical shift anisotropy (CSA) relaxation mechanism plays a minor role (<20%). Under these conditions ^{13}C T_1 and NOE are expressed in terms of the spectral density function $J(\omega)$ in the following equations.[33−35]

$$\frac{1}{T_1} = \frac{1}{T_1^{DD}} + \frac{1}{T_1^{CSA}} \tag{1}$$

$$NOE = 1 + \frac{NOE^{DD} - 1}{(1/T_1^{DD} + 1/T_1^{CSA})T_1^{DD}} \tag{2}$$

where

$$\frac{1}{T_1^{DD}} = Kn[J(\omega_H - \omega_C) + 3J(\omega_C) + 6J(\omega_H + \omega_C)] \tag{3}$$

$$\frac{1}{T_1^{CSA}} \cong \frac{2}{15}\omega_c^2(\sigma_1 - \sigma_2)^2 J(\omega_c) \tag{4}$$

$$NOE^{DD} = 1 + \frac{\gamma_H}{\gamma_C}\left[\frac{6J(\omega_H + \omega_C) - J(\omega_H - \omega_C)}{J(\omega_H - \omega_C) + 3J(\omega_C) + 6J(\omega_H + \omega_C)}\right] \tag{5}$$

In these expressions, $\omega_H/2\pi$ and $\omega_C/2\pi$ are Larmor frequencies of ^1H and ^{13}C nuclei, n is the number of protons directly bonded to the carbon of interest, γ_H and γ_C are the gyromagnetic ratios of ^1H and ^{13}C, and K is a constant which depends on the $^1H-^{13}C$ bond length.[34] In the expression for T_1^{CSA}, σ_1 and σ_2 denote chemical shifts parallel and perpendicular to the symmetry axis of chemical shift tensor. We have chosen $\sigma_1 - \sigma_2 = 150$ ppm for PI carbon 3 and $\sigma_1 - \sigma_2 = 0$ ppm for PI carbons 1 and 4 under the approximation that the symmetry axis of chemical shift lies along the $^{13}C-H$ bond. Since CSA is a minor relaxation mechanism, this is not a significant approximation. Note that eqs 1−5 are valid for an isotropic system.[36]

Deuterium relaxation is dominated by the electric quadrupole coupling of deuterium nuclei and has the following relationship to the reorientation of a C−D bond.[37]

$$\frac{1}{T_1} = \frac{3}{10}\pi^2(e^2qQ/h)^2[J(\omega_D) + 4J(2\omega_D)] \tag{6}$$

Here $\omega_D/2\pi$ is the Larmor frequency of deuterium. The ^2H quadrupole coupling constant e^2qQ/h was taken as 172 and 190 kHz for backbone and side group deuterons, respectively.[37]

In all above expressions, $J(\omega)$ is the spectral density function and is the Fourier transform of the orientation autocorrelation function, $G(t)$, for the C−H or C−D bond of interest:

$$J(\omega) = {}^1/_2\int_{-\infty}^{\infty} G(t)\exp(-i\omega t)\,dt \tag{7}$$

$G(t)$ is the object of our interest because it describes the dynamics of individual C−H and C−D bonds:

$$G(t) = {}^3/_2\langle\cos^2\theta(t)\rangle - {}^1/_2 \tag{8}$$

Here $\theta(t)$ is the angle of a C−H or C−D bond relative to its orientation at time $t = 0$. Since $G(t)$ is not directly observable in these NMR measurements, we proceed by assuming a particular functional form for $G(t)$ and then optimize the fitting parameters by comparison with the experimental data.

Correlation Function and Correlation Time. The modified KWW function (mKWW) has recently been shown to give an excellent representation of the C−H vector autocorrelation function for atactic polypropylene,[35,38] and we employ it here as well.

$$G(t) = a_{lib}\exp\left(\frac{-t}{\tau_{lib}}\right) + (1 - a_{lib})\exp\left(-\left(\frac{t}{\tau_{seg}}\right)^{\beta}\right) \tag{9}$$

This function indicates that C−H vector reorientation occurs by two mechanisms: librational motion and segmental dynamics. Here a_{lib} and τ_{lib} are the amplitude and relaxation time for librational motion. Fits to the experimental data are insensitive to τ_{lib}, and this quantity is set equal to 1 ps. τ_{seg} and β describe the distribution of relaxation times associated with segmental dynamics. We assume that τ_{seg} has a VTF (or WLF) temperature dependence:[3,14,39]

$$\log\left(\frac{\tau_{seg}}{\tau_\infty}\right) = \frac{B}{T - T_0} \tag{10}$$

where τ_∞, B, and T_0 are constants for a given component in a particular blend. Often we are interested in the correlation time for segmental dynamics $\tau_{seg,c}$ which we define as the integral of the segmental portion of the correlation function:

$$\tau_{seg,c} = \frac{\tau_{seg}}{\beta}\Gamma\left(\frac{1}{\beta}\right) \tag{11}$$

Results

Figures 1−4 show measured ^{13}C T_1 and NOE values for pure polyisoprene and the PI component in the blended samples. Note that the T_1 minimum at 125.9 MHz moves to successively higher temperatures as the weight fraction of dPVE is increased. Since the T_1 minimum indicates the temperature at which segmental dynamics occur on roughly a 1 ns time scale, this qualitatively indicates that PI dynamics slow down as dPVE is added to the blend. For the 30/70 PI/dPVE sample, the T_1 minimum has shifted about 20 K compared with pure PI. For all samples, the methine carbon has lower values of nT_1 at the T_1 minimum than do the methylene carbons; this is consistent with a nonnegligible CSA contribution for the methine carbon. NOE values also show that PI dynamics slow as PVE

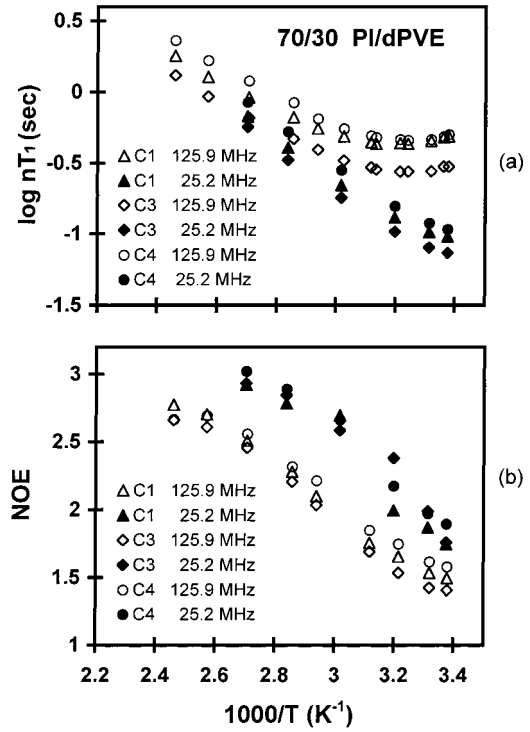

Figure 2. ^{13}C NMR relaxation time measurements for PI backbone carbons in the 70/30 PI/dPVE blend.

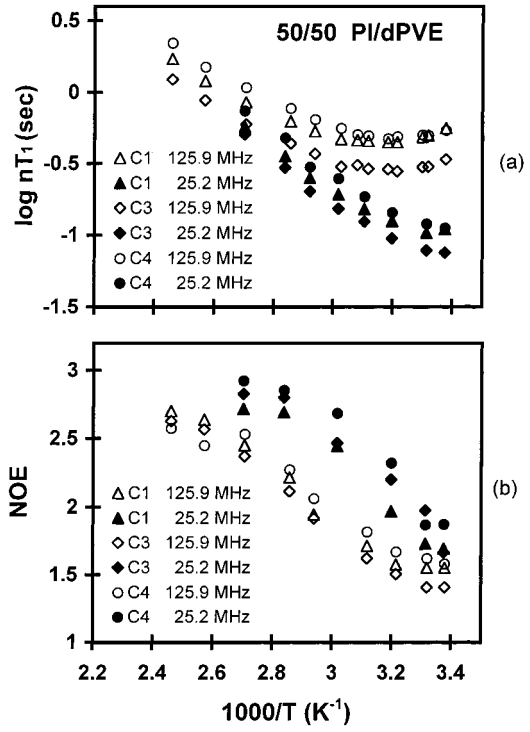

Figure 3. ^{13}C NMR relaxation time measurements for PI backbone carbons in the 50/50 PI/dPVE blend.

is added to the blend. For example, for pure PI, NOE values at 125.9 MHz do not reach their minimum value while this minimum is attained for the 50/50 blend.

Figure 5 shows rate-averaged ^{2}H T_1 values of pure dPVE and dPVE in blends with PI. Clearly, the T_1 minima at both frequencies are moving toward low temperature as PI component is added, qualitatively indicating that dPVE dynamics become faster with blending. For the 70/30 blend, which has largest PI

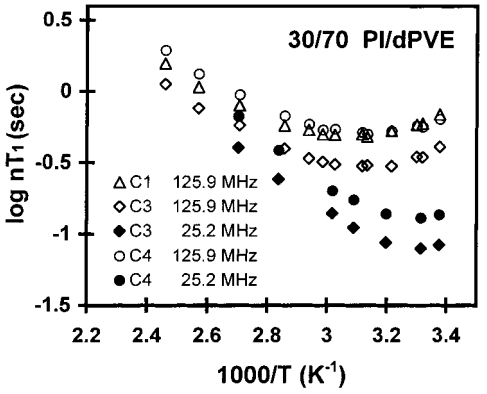

Figure 4. ^{13}C NMR relaxation time measurements for PI backbone carbons in the 30/70 PI/dPVE blend.

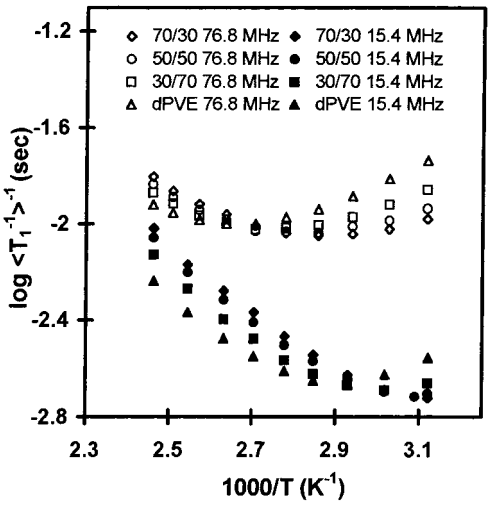

Figure 5. ^{2}H T_1 for dPVE component in pure dPVE and blends (e.g., 70/30 = 70 wt % PI). As described in the text, the rate average T_1 for the six deuterons in dPVE is presented.

content, the T_1 minimum moved about 30 K toward low temperature compared with the case of pure dPVE.

Superposition of the Experimental Data. One way to examine the effect of blending upon segmental dynamics is to directly superpose the experimental data using temperature shifts. As shown in Figure 6, we found that temperature shifts (not shifts in $1/T$) produced quite satisfactory master curves. Small vertical shifts were needed to superpose the T_1 data. All the shift parameters are listed in Table 3. A strong indication that these shifts are meaningful is the fact that the same temperature shifts sufficed to superpose both the T_1 and NOE data at two different fields (for the PI component). In addition, the same shifts sufficed to superpose the data from all three PI backbone carbons (not shown). The superposition procedure used here is similar to that used by Lauprêtre et al.[18]

Fitting to mKWW and VTF Functions. Although the superposition procedure provides some information about the effects of blending on the component dynamics, fitting the relaxation time data to a model correlation function allows a more quantitative description of the experimental results. As we show below, this model-dependent fitting procedure produces results in good agreement with the model-independent shift technique. Since we found in a previous study that the mKWW function (eq 9) provides a superior fit to NMR relaxation time data, we employ it here as well, in combination with the assumption of a VTF temperature dependence

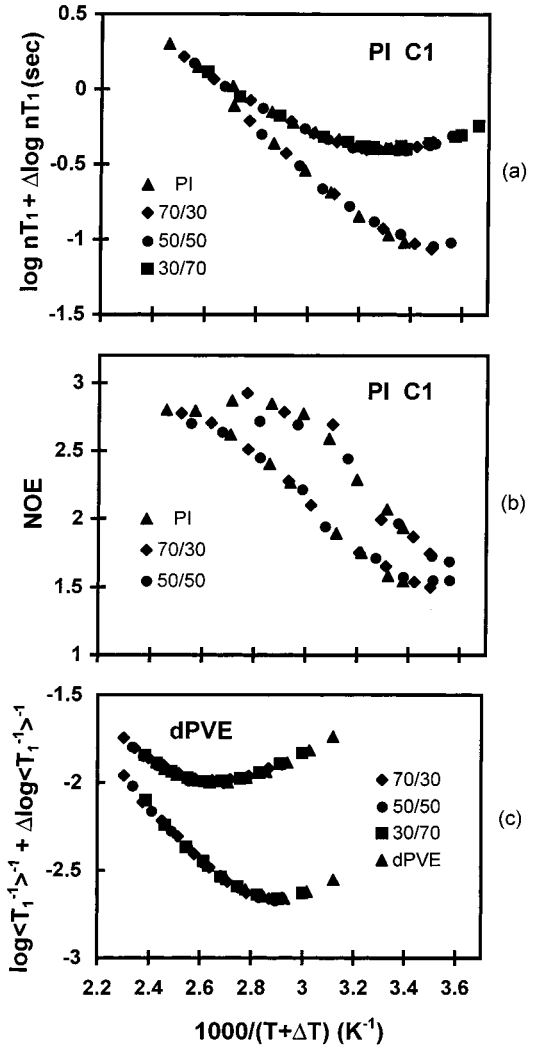

Figure 6. Superposition of data for melts and blends: (a) ^{13}C T_1 for PI carbon 1; (b) NOE of PI carbon 1; (c) ^2H T_1 for dPVE component. For both PI and dPVE, a single temperature shift suffices to superpose all the data for a given blend composition with data for pure melts of the individual components. For PI, the same temperature shift superposed data for all three backbone carbons. In the case of panels a and c, very small vertical shifts were also performed. Shift parameters are given in Table 3.

Table 3. Horizontal and Vertical Shifts Needed To Superpose Experimental Data of Blends onto Those of Pure Samples

components	samples	ΔT (K)	$\Delta\log(nT_1)$ (s)	ΔT_0 (K)[a]
PI	70/30	−9	−0.03	−8
	50/50	−14	−0.05	−13
	30/70	−21	−0.07	−22
dPVE	30/70	13	0.03	14
	50/50	22	0.04	25
	70/30	28	0.06	27

[a] From fits in Table 4.

(eq 10). Fitting was performed individually on the experimental data set for each nucleus in each blend using eqs 1−10. For each of the three carbons of PI, ^{13}C T_1 and NOE at both frequencies and all temperatures were taken and fitted simultaneously. In this procedure, there are five unknown parameters: a_{lib}, β, τ_∞, B, and T_0. Because of the relatively small range of correlation times sampled in these measurements, B and T_0 are highly correlated with each other, and one of these two parameters needed to be constrained for all samples to produce reasonable trends in terms of blending; we chose to constrain B for each nuclei. In addition to this, a_{lib} for a given C−H vector was constrained for all samples because the proportion of libration was considered to be unchanged by the environment of molecules.[40] As shown for the examples in Figure 7, this procedure yielded excellent fits to the experimental data. Fitting parameters are given in Table 4.

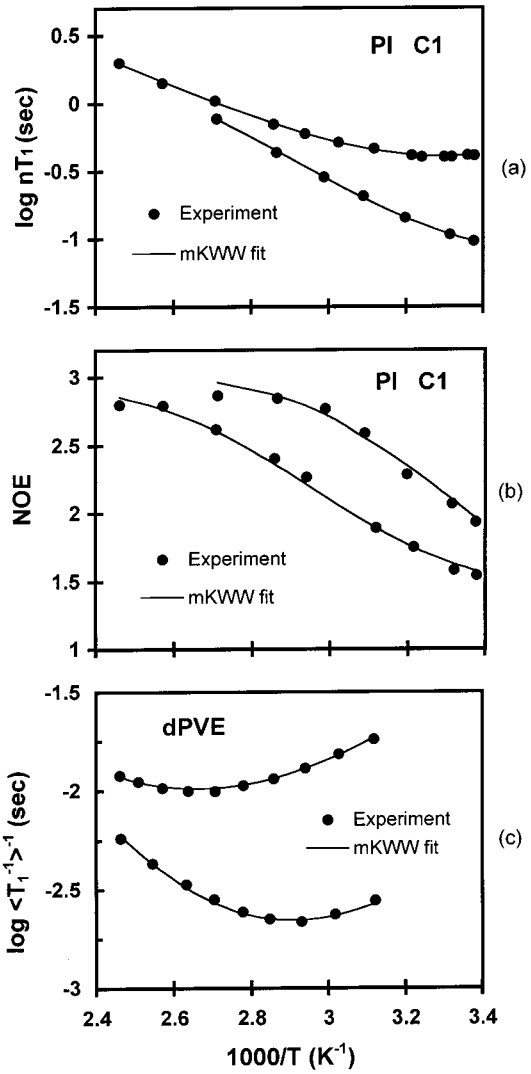

Figure 7. Representative fitting results: (a) ^{13}C T_1 for carbon 1 of pure PI, (b) NOE for carbon 1 of pure PI, and (c) ^2H T_1 for dPVE. Each fit utilized a modified Kohlrausch−Williams−Watts form for the correlation function and a VTF temperature dependence. Data in panels a and b were fit simultaneously.

A similar fitting procedure was used for the dPVE data with one exception. We were unable to obtain a good fit to the experimental data for dPVE without allowing β to change slightly with temperature. β was taken to increase linearly with increasing temperature over the range shown in Table 4. This is likely required because correlation times for different C−D vectors in dPVE have slightly different temperature dependencies[41] but are being lumped together in our fits.

Calculated Correlation Times. From the fitting parameters in Table 4, the correlation times of PI and dPVE dynamics were calculated using eq 11. Because the correlation times of the three different carbons in PI were very similar for any temperature within the range of the experiments, these were averaged and the

Table 4. Best Fit Parameters for Segmental Dynamics of PI and DPVE (See Eqs 9 and 10)

		samples				
		pure PI	70/30	50/50	30/70	pure dPVE
PI dynamics						
C_1	β	0.52	0.47	0.45	0.42	
B: 425 K	τ_∞ (ps)	0.197	0.167	0.150	0.138	
a_{lib}: 0.30	T_0 (K)	174	182	188	196	
C_3	β	0.60	0.56	0.54	0.50	
B: 459 K	τ_∞ (ps)	0.368	0.333	0.309	0.280	
a_{lib}: 0.22	T_0 (K)	174	181	187	194	
C_4	β	0.49	0.46	0.43	0.40	
B: 446 K	τ_∞ (ps)	0.164	0.132	0.121	0.099	
a_{lib}: 0.32	T_0 (K)	173	183	187	197	
average	β	0.54	0.50	0.47	0.44	
B: 443 K	τ_∞ (ps)	0.24	0.21	0.19	0.17	
a_{lib}: 0.28	T_0 (K)	174	182	187	196	
dPVE dynamics						
B: 470 K	β		0.48	0.49−0.45	0.49−0.42	0.46−0.37
a_{lib}: 0.3	τ_∞ (ps)		1.08	1.18	1.06	0.93
	T_0 (K)		186	188	199	213

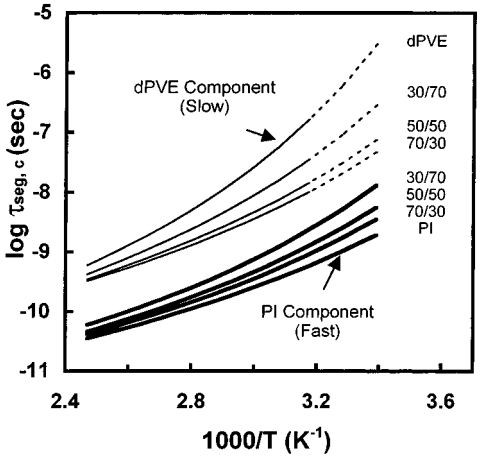

Figure 8. Segmental correlation times for both components in PI/dPVE blends at various compositions. Solid lines are the results of fits to the modified KWW correlation function and a VTF temperature dependence. The dashed lines represent extrapolations based on fitted VTF parameters. Even at these high temperatures, the dynamics of the components in a given blend are not equal. For polyisoprene, the plotted lines represent the average behavior of the three (very similar) backbone carbons.

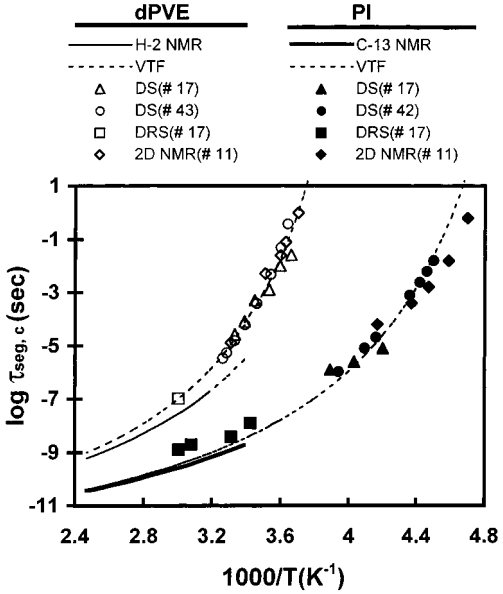

Figure 9. Comparison of segmental correlation times for pure PI and dPVE with previous work. The curves labeled "VTF" were calculated from the parameters obtained by fitting our data after shifting T_0 to account for T_g differences (shift for PI = 8 K, shift for dPVE = 15 K). After this shift, reasonable agreement is obtained between the present results at high temperature and previous work at lower temperature.

average values are used for further discussion. (The average correlation times are essentially equal to the ones calculated from averaging the parameters given in Table 4.) The similarity of the correlation times for these three carbons is expected and is one indication of the robustness of the fitting procedure. Another indication is the excellent agreement for both PI and dPVE between the shifts in T_0 due to blending and the temperature shifts deduced from the superposition procedure (see comparison in Table 3).

Figure 8 shows the correlation times for PI and dPVE as a function of temperature in pure samples and blends. As expected, the correlation times of PI at a given temperature increase as dPVE is added; this is more pronounced at low temperature. The correlation times of PI show an obviously non-Arrhenius temperature dependence even in this high-temperature range. For the dPVE component, whose correlation times also have a non-Arrhenius temperature dependence, dynamics become much faster as the PI component is added. Though the qualitative shapes of the correlation time curves are the same for dPVE and PI, the slopes are steeper for dPVE, indicating a higher apparent activation energy for this component in a given blend.

Comparison with Other Work on Pure PI and PVE Melts. Before discussing component dynamics in PI/PVE blends, we compare the dynamics of the pure components, as deduced in this study, with other work on pure PI and PVE homopolymers; blend results are discussed in the next section. Low molecular weight polymers were chosen for this study to allow a rigorous comparison with MD computer simulations. Comparison of our results with other work on high molecular weight polymers allows some indication of the effect of molecular weight on the dynamics of PI and PVE.

Figure 9 shows correlation times for segmental dynamics of pure PI and PVE from five sources including this study.[11,17,42,43] Two curves are plotted for our data for each homopolymer; one corresponds to the parameters in Table 4 while for the other we have adjusted the T_0 value by the differences in T_g between our low molecular weight samples and those obtained for high

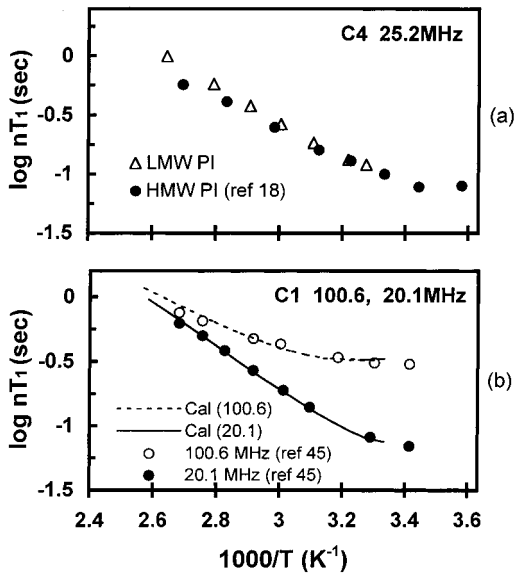

Figure 10. Comparison of ^{13}C T_1 between high and low molecular weight PI: (a) comparison with data in ref 18 at 25.2 MHz; (b) comparison of calculated ^{13}C T_1 for low molecular weight PI in present study with data from ref 45. For both panels, our data has been shifted by 9 K to account for the T_g difference between the high and low molecular weight samples. The reasonable agreement indicates that, after the temperature shift due to T_g, dynamics are very similar in high and low molecular weight PI.

molecular weight samples. All other data in the figure were obtained with high molecular weight samples, with the exception of the PVE data from ref 17. All dielectric spectroscopy (DS) and depolarized Rayleigh scattering (DRS; Fabry−Perot interferometry) results have been evaluated accounting for the β parameter, as in eq 11.

With the exception of the DRS results for PI, all the data shown in Figure 9 are reasonably consistent, after accounting for the T_g differences. The relaxation time measured by DRS is associated with the reorientation of the polarizability tensor. Apparently, this relaxation involves a larger portion of the chain than the conformational dynamics which are measured in the NMR experiment.[44]

In Figure 10 we show an additional check which can be made between our results for PI and those from previous NMR relaxation times experiments using higher molecular weight PI.[18,45] In each case, our results are quite consistent with the previous work if a 9 K temperature shift is introduced to account for the T_g differences; this temperature shift has been incorporated into the data in the figure. In Figure 10b, a direct comparison with the previous work could not be made because the data were acquired at different frequencies. We have used the fits to our data (Table 4) to calculate the relaxation times expected at 20.1 and 100.6 MHz, and these are plotted as lines in this panel.

The comparisons in Figures 9 and 10 argue strongly that the low molecular weight PI and PVE used in the present study have segmental dynamics which are very similar to those of high molecular weight samples after accounting for the differences in T_g.

Intrinsic Mobility Differences in PI/PVE Blends. We can use the information on component dynamics shown in Figure 8 in several ways. Figure 11 shows, for two different temperatures, the influence of blend composition on the dynamics of each component. Of particular interest are the two curves for 405 K. The

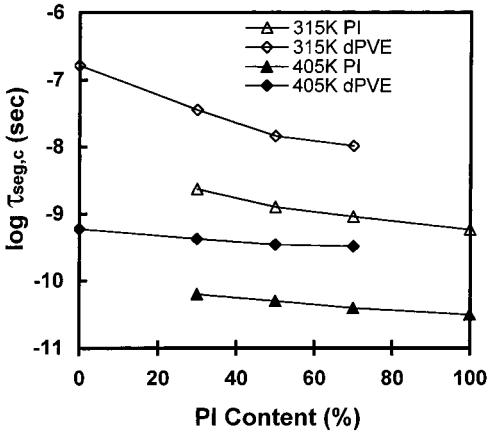

Figure 11. Isothermal correlation time changes caused by blending. At high temperature, the difference between the two curves together with the weak composition dependence implies a substantial intrinsic mobility difference between PI and dPVE chains.

dynamics of PI and dPVE change very little as the composition is varied, indicating that each chain cares little about its environment at this high temperature. At the same time, the segmental dynamics of the two chains differ by a factor of 6, indicating that there is a substantial intrinsic mobility difference between PI and dPVE chains; i.e., in exactly the same environment, the segmental dynamics of dPVE chains are considerably slower than those of PI. This effect is not generally included in models of blend dynamics but clearly is of substantial importance. The intrinsic mobility difference might be even more important at lower temperature. Kornfield et al. concluded that models which did not include intrinsic mobility differences could not fit PI/PVE data near T_g.[9]

We interpret the factor of 6 intrinsic mobility difference at 405 K as being the difference due to molecular structure and intramolecular potentials. (Doxastakis et al. have previously pointed out the necessity of high-temperature measurements for understanding the effect of molecular structure on blend dynamics.[17]) Qualitatively, the faster dynamics observed for PI are reasonable given the absence of a side group and the lower barriers for internal rotation[46] (for two of the three backbone torsions). If this reasoning is correct, then a similar intrinsic mobility difference should be observed for PI and dPVE in dilute solution in low molecular weight solvents. Indeed, this is the case. The segmental dynamics of PI and dPVE have been measured in a number of solvents.[47,48] In toluene at 333 K, the correlation time for segmental dynamics for PI is 5.9 times faster than that of dPVE. A factor of 6.3 is observed in hexadecane at 360 K. From the observed dependence of the correlation times on temperature, one would expect the same ratio for measurements at 405 K.

At 315 K, Figure 11 shows that the difference between the segmental dynamics of the two chains at a given blend composition is even larger than that observed at 405 K. However, this cannot directly be interpreted as an intrinsic mobility difference. In a blend with 50/50 overall composition, PI segments will find themselves on average surrounded by more PI segments than PVE segments. This "self-concentration" effect[9] results from chain connectivity. For example, two nearest-neighbor segments surrounding any PI segment must also be PI segments for all blend compositions. Since both chains

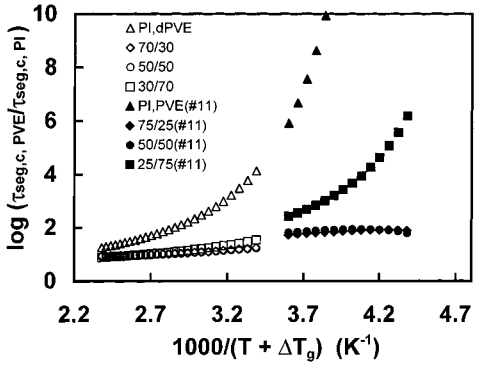

Figure 12. Ratio of correlation times of dPVE and PI components in pure melts (upper curve) and blends (bottom three curves). Open symbols are from the present study while filled symbols are from the solid-state NMR results of Kornfield and co-workers (ref 11). A temperature shift in the horizontal axis accounts for T_g differences ($\Delta T_g = 15$ K).[9]

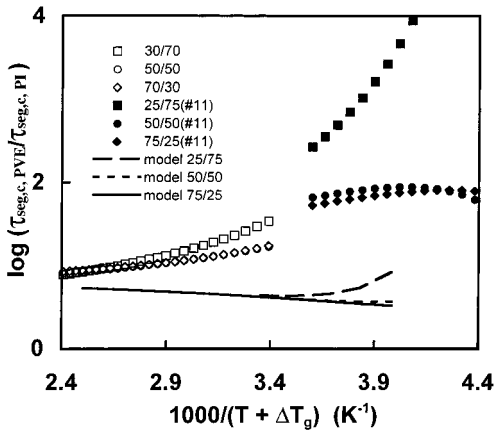

Figure 13. Ratio of correlation times of dPVE and PI components in blends compared to prediction of the model of Kumar et al. (ref 15).

at 315 K show substantial mobility changes with composition, part of the difference in mobility at any given average composition can be ascribed to this self-concentration effect. Thus, the intrinsic mobility difference between PI and dPVE can only be extracted at this temperature through the use of a model.

Comparison with Lower Temperature Experiments on PI/PVE Blends. Kornfield and co-workers have used solid-state ^{2}H NMR to investigate the component dynamics of PI/PVE blends at temperatures near T_g.[9,11,13] These experiments are also sensitive to the reorientation of C−D vectors and thus are of special interest for comparison to our work. Figure 12 shows a comparison of results from the Kornfield's group (right side) and the results presented here (left side). For all curves, the segmental correlation time for PVE is divided by the segmental correlation time for PI. The triangles show this ratio for the two pure homopolymers, while the other symbols show this ratio for the two components in a particular blend. It is apparent that the two data sets fit together reasonably well.

First we consider the qualitative interpretation of this plot and then, in the following paragraph, consider some important aspects of its construction. If PI and PVE chains in a given blend cared only about their own identity and not at all about their environment, then the results for the blends should line up with the ratio observed for the two homopolymers. If, on the other hand, the two chains are forced to relax at the same rate due to their intimate contact, then the results for the blends should lie on the lower horizontal axis of the graph. Clearly neither of these extreme scenarios describes the blend data. Although mixing causes very substantial changes in the dynamics of each component, the ratio of segmental relaxation times for the two components is still large, varying from 1 decade to more than 3 decades, depending upon temperature and composition.

The construction of this plot requires some comments and caveats: (1) A temperature shift was introduced into our data in order to account for the T_g difference between the samples ($\Delta T_g = 15$ K).[9] This temperature shift may not account for all effects of the molecular weight differences. However, on the assumption that any dynamic correlation length at high temperature would be quite small (and therefore smaller than the static correlation length for both samples), the difference in static correlation lengths for high and low molecular weight blends would not be expected to influence the results of our experiments. (2) We assume that deuteration has no influence on segmental dynamics. (3) All the points plotted are the results of fits to data and are not directly measured data points. For our data, this procedure is required since correlation times are only obtained by fitting data at many temperatures. For Kornfield's data, this procedure is used since the temperature range where the dynamics of both components can be measured is considerably smaller than the temperature range shown. Thus, the slight misfit between the two data sets should be considered in this light. (4) Slightly different compositions were studied; thus, we compare PI/PVE 75/25 to a 70/30 sample without attempting to account for the composition difference.

Comparison to Kumar/Colby Model. Figure 12 shows a combined data set characterizing component dynamics in PI/PVE blends over a 200 K temperature range. One goal of this study was to provide such a data set for comparison with various models of blends dynamics. Here we illustrate the utility of these data by making comparison to the recent work of Kumar et al.[15] The physical picture behind this model is that each segment has a relaxation time which depends on the local composition; environments rich in the high-T_g material naturally give rise to slower segmental dynamics. In addition, a self-concentration term biases the local composition. The definition of "local" is critical for this and related approaches.[28] Kumar et al. take the size of this region to be dependent upon both temperature and local composition so as to reflect the distance from T_g. For these calculations, the model of Donth provides the required temperature dependence.[49]

Figure 13 shows a comparison between the combined data set and the model of Kumar et al. for the ratio of component dynamics in the blend. The model calculations were performed for the molecular weights used in the Kornfield experiments; at high temperatures, the model predictions are independent of molecular weight. The model clearly fails quantitatively. Qualitatively, the model correctly predicts that segmental dynamics for the two components are more disparate in blends rich in PVE. For the two other blend compositions, the model predicts that lowering temperature lessens the ratio of component correlation times, in contrast to the experimental data. Of course, the ratio of component relaxation times is only one possible way of plotting the

experimental results. Reference 15 shows that this model is more successful in other types of comparisons with data for the PI/PVE blend.

Comparison to Other Work on PI/PVE at High Temperature. Recently, a number of publications[14,17,18,50] on component dynamics in PI/PVE blends at high temperature have appeared. Quasi-elastic neutron scattering (QENS) have been reported by Doxastakis et al. (PI/PVE = 70/30) and by Hoffmann et al. (PI/PVE = 50/50).[17,50] In these experiments, the relaxation times associated with translational motion of each component are measured as a function of wave vector Q. Since the orientational correlation function measured by NMR has no wave vector associated with it, it is not obvious how best to compare these two types of experiments. Hoffman et al. found that in the segmental dynamics regime the pure components and the components in the blend all had a similar dependence on Q. Thus, in this regime, the change in segmental dynamics due to blending is independent of Q and can be compared to our results. Qualitative agreement with our results are found. At 330 K, ref 50 reports the difference in dynamics between the blend components for a 50/50 blend as 0.7 decade while our results indicate a difference of about 1.0 decade. For the 70/30 blend studied in ref 17, the comparison is not as favorable; they report a difference of 0.35 decade between the dynamics of the two components in the blend while our results again indicate 1.0 decade. Given the different nature of the observables, it is not clear that these results constitute disagreement. This is certainly a point where realistic MD computer simulations would provide some insight.

Adams and Adolf recently utilized fluorescence anisotropy decay measurements to measure component dynamics of anthracene-labeled PI and PVE in PI/PVE blends.[14] While the qualitative features of their data are similar to those presented here, our results are not in good quantitative accord with the results of ref 14. For example, our results show larger changes in relaxation times with composition and also a bigger difference between the dynamics of the two components. The sensitivity of the fluorescence anisotropy method allowed the study of dilute chains of one component in a matrix of the other component which allowed mixing rules to be evaluated. The exploration of the dynamics of dilute chains in a blend is an important contribution which seems likely to be useful in future studies.

Changes in Distribution Width with Blending. The fits reported in Table 4 indicate some small changes in the distribution of relaxation times associated with blending, as indicated by changes in the KWW β parameter. For dPVE, because all the C−D vectors have been fit simultaneously, these changes (and the changes with temperature) should not be considered significant. For PI, the fits for each carbon consistently indicate a tendency toward broadening the distribution of relaxation times as dPVE is added. The PI data can also be fit by constraining β to remain constant and allowing the fraction of the correlation function decay associated with libration (a_{lib}) to increase with blending. We favor the former explanation for physical reasons since the required changes in a_{lib} are quite large (e.g., from 0.28 to 0.43). Nevertheless, we can only conclude that the data suggest some small broadening of the relaxation time distribution for the PI component as dPVE is added. These two different procedures for fitting the PI data result in essentially identical correlation times for the segmental dynamics of the two components (maximum deviation is 0.1 decade).

Concluding Remarks

We have investigated the segmental dynamics of each component in low molecular weight PI/dPVE blends. For both components, the orientation autocorrelation for C−H or C−D vectors is well described by a Kohlrausch−Williams−Watts function with an additional fast component to account for librational motion. Correlation time changes obtained in this way agree well with those inferred from a model-independent superposition approach. The data obtained here in the high-temperature regime are reasonably consistent with the low-temperature results presented by Kornfield et al. and together provide a data set covering T_g to $T_g + 200$ K over a range of compositions. The combined data set provides a rigorous test for models of blend dynamics. As an example, comparisons were made to the model of Kumar et al.[15] Some qualitative features of the experimental results were not reproduced by the model.

The data indicate a substantial intrinsic mobility difference of nearly 1 order of magnitude between PI and dPVE chains far above T_g. Intriguingly, for this blend system, this intrinsic mobility difference is in quantitative agreement with measurements of each chain individually as a dilute component in a common solvent. This suggests that the origin is entirely intramolecular and that blends with a larger dynamic contrast (ΔT_g) may show even larger intrinsic mobility differences. Future experiments will test this possibility.

Acknowledgment. This research was supported by the National Science Foundation through the Division of Material Research, Polymer Program (DMR-0099849). We thank Ping Tong for performing DSC measurements, Ralph Colby and Sanat Kumar for helpful discussions, and Sanat Kumar for providing calculations for the model of ref 15. Measurements were performed at the Instrument Center of the Department of Chemistry, University of Wisconsin−Madison, supported by NSF CHE-8306121 and NIH 1 S10 RR02388-01. We thank Charles Fry and Marvin Kontney for their support.

References and Notes

(1) Paul, D. R.; Newman, S. *Polymer Blends*; Academic Press: New York, 1978; Vol. 1.
(2) Pathak, J. A.; Colby R. H.; Floudas, G.; Jerome, R. *Macromolecules* **1999**, *32*, 2553.
(3) Arendt, B. H.; Krishnamoorti, R.; Kornfield, J. A.; Smith, S. D. *Macromolecules* **1997**, *30*, 1127.
(4) Roland, C. M. *Macromolecules* **1987**, *20*, 2557.
(5) Roland, C. M. *J. Polym. Sci., Polym. Phys. Ed.* **1988**, *26*, 839.
(6) Trask, C. A.; Roland, C. M. *Macromolecules* **1989**, *22*, 256.
(7) Miller, J. B.; McGrath, K. J.; Roland, C. M.; Trask, C. A.; Garroway, A. N. *Macromolecules* **1990**, *23*, 4543.
(8) Tomlin, D. W.; Roland, C. M. *Macromolecules* **1992**, *25*, 2994.
(9) Chung, G. C.; Kornfield, J. A.; Smith, S. D. *Macromolecules* **1994**, *27*, 964.
(10) Alegría, A.; Colmenero, J.; Ngai, K. L.; Roland, C. M. *Macromolecules* **1994**, *27*, 4486.
(11) Chung, G. C.; Kornfield, J. A.; Smith, S. D. *Macromolecules* **1994**, *27*, 5729. Saxena. S.; Cizmeciyan, D.; Kornfield, J. A. *Solid State NMR* **1998**, *12*, 165.
(12) Roovers, J.; Toporowski, P. M. *Macromolecules* **1992**, *25*, 3454.
(13) Alvarez, F.; Alegría, A.; Colmenero, J. *Macromolecules* **1997**, *30*, 597.
(14) Adams, S.; Adolf, D. B. *Macromolecules* **1999**, *32*, 3136.
(15) Kumar, S. K.; Colby, R. H.; Kamath, S.; Pathak, J. A. Submitted to *J. Chem. Phys.* Kamath, S.; Colby, R. H.;

Kumar, S. K.; Karatasos, K.; Floudas, G.; Fytas, G.; Roovers, J. E. L. *J. Chem. Phys.* **1999**, *111*, 6121.
(16) Arbe, A.; Alegría, A.; Colmenero, J.; Hoffmann, S.; Willner, L.; Richter, D. *Macromolecules* **1999**, *32*, 7572.
(17) Doxastakis, M.; Kitsiou, M.; Fytas, G.; Theodorou, D. N.; Hadjichristidis, N.; Meier, G.; Frick, B. *J. Chem. Phys.* **2000**, *112*, 8687. The depolarized Rayleigh scattering relaxation times which are reported in this paper are too long by a factor of 2π (Fytas, G., private communication).
(18) Lauprêtre, F.; Monnerie, L.; Roovers, J. *PMSE Prepr.* **2000**, *82*, 154.
(19) Katana, G.; Fischer, E. W.; Hack, T.; Abetz, V.; Kremer, F. *Macromolecules* **1995**, *28*, 2714.
(20) Chin, Y. H.; Zhang, C.; Wang, P.; Inglefield, P. T.; Jones, A. A.; Kambour, R. P.; Bendler, J. T.; White, D. M. *Macromolecules* **1992**, *25*, 3031.
(21) Se, K.; Takayanagi, O.; Adachi, K. *Macromolecules* **1997**, *30*, 4877.
(22) Sy, J. W.; Mijovic, J. *Macromolecules* **2000**, *33*, 933.
(23) Rizos, A. K.; Fytas, G.; Semenov, A. N. *J. Chem. Phys.* **1995**, *102*, 6931.
(24) Cendoya, I.; Alegria, A.; Alberdi, J. M.; Colmenero, J.; Grimm, H.; Richter, D.; Frick, B. *Macromolecules* **1999**, *32*, 4065.
(25) Bergquist, P.; Shi, J. F.; Zhao, J.; Jones, A. A.; Inglefield, P. T.; Kambour, R. P. *Macromolecules* **1998**, *31*, 3632.
(26) McGrath, K. J.; Roland, C. M. *J. Non-Cryst. Solids* **1994**, *172*−*174* (Pt. 2), 891.
(27) Kumar, S. K.; Colby, R. H.; Anastasiadis, S. H.; Fytas, G. *J. Chem. Phys.* **1996**, *105*, 3777.
(28) Lodge, T. P.; MacLeish, T. C. B. *Macromolecules* **2000**, *33*, 5278.
(29) Zetsche, A.; Fischer, E. W. *Acta Polym.* **1994**, *45*, 168.
(30) Hadjichristidis, N.; Iatrou, H.; Pispas, S.; Pitsikalis, M. *J. Polym. Sci., Polym. Chem. Ed.* **2000**, *38*, 3211.
(31) Ramzi, A.; Prager, M.; Richter, D.; Efstratiadis, V.; Hadjichristidis, N.; Young, R. N.; Allgaier, J. B. *Macromolecules* **1997**, *30*, 7171.
(32) Bywater, S.; Mackerron, D. H.; Worsfold, D. J. *J. Polym. Sci., Polym. Chem. Ed.* **1985**, *23*, 1997.
(33) Dais, P.; Spyros, A. *Prog. Nucl. Magn. Reson. Spectrosc.* **1995**, *27*, 555.
(34) Gisser, D. J.; Glowinkowski, S.; Ediger, M. D. *Macromolecules* **1991**, *24*, 4270.
(35) Moe, N. E.; Qiu, X. H.; Ediger, M. D. *Macromolecules* **2000**, *33*, 2145.
(36) Qiu, X. H.; Ediger, M. D. *J. Polym. Sci., Polym. Phys. Ed.* **2000**, *38*, 2634. See Appendix I for details of the derivation of eqs 1−5 for an isotropic system.
(37) Zhu, W.; Ediger, M. D. *Macromolecules* **1995**, *28*, 7549.
(38) Qiu, X. H.; Moe, N. E.; Ediger, M. D.; Fetters, L. J. *J. Chem. Phys.* **2000**, *113*, 2918.
(39) Angell, C. A. *Polymer* **1997**, *38*, 6261.
(40) An alternate procedure, that of constraining β, has been adopted in ref 18. We also fit our data with this assumption and discuss our findings at the end of the Discussion section.
(41) This point was confirmed by ^{13}C NMR measurements at two frequencies on a high molecular weight PVE sample. Because the microstructure of this sample was different from that of the dPVE sample, a quantitative comparison between the two data sets is difficult. Qualitatively, the two data sets are consistent.
(42) Boese, D.; Kremer, F. *Macromolecules* **1990**, *23*, 829.
(43) Hofmann, A.; Alegría, A.; Colmenero, J.; Willner, L.; Buscaglia, E.; Hadjichristidis, N. *Macromolecules* **1996**, *29*, 129.
(44) Lindsey, C. P.; Patterson, G. D.; Stevens, J. R. *J. Polym. Sci., Polym. Phys. Ed.* **1979**, *17*, 1547.
(45) Denault, J.; Prud'homme, J. *Macromolecules* **1989**, *22*, 1307.
(46) Adolf, D. B.; Ediger, M. D. *Macromolecules* **1991**, *24*, 5834.
(47) Glowinkowski, S.; Gisser, D. J.; Ediger, M. D. *Macromolecules* **1990**, *23*, 3520.
(48) Zhu, W.; Ediger, M. D. *Macromolecules* **1995**, *28*, 7549.
(49) Donth, E. J. *Non-Cryst. Solids* **1992**, *53*, 325.
(50) Hoffmann, S.; Willner, L.; Richter, D.; Arbe, A.; Colmenero, J.; Farago, B. *Phys. Rev. Lett.* **2000**, *85*, 772.

MA0018345